Available online at www.sciencedirect.com
SCIENCE DIRECT®

Nuclear Science and Techniques, Vol.17, No.1 (2006) 34–37

NUCLEAR SCIENCE AND TECHNIQUES

Energy deposition of γ-ray in different instances and its influence on energy detection

TANG Shi-Biao [1, *] MA Qing-Li [1] KONG Le [1] YIN Ze-Jie [1] HUANG Huan [1]
ZHU Da-Ming [2]

[1](Department of Modern Physics, University of Science and Technology of China, Hefei 230026, China)

[2](Department of Physics, University of Missouri-Kansas City, Kansas City, Missouri 64110, USA)

Abstract In this paper, we simulate γ-ray energy deposition for different incident energies with four different models using the tool GEANT4（Geant4.7.0, 2005）developed by CERN (the Center of European Research of Nucleus). The results we obtained indicate that there are different peak values for different incident energies. That is, we can differentiate the incident energy accurately if the detector can determine the peak value accurately. This is meaningful for the geometrical configuration of the detector to get the most probable distribution (MPD) of energy deposition for different incident energies. According to the simulation, we can insert certain slices with large absorption coefficient to obtain a better MPD of energy deposition which will not alter the shape of the energy deposition.

Key words GEANT4, Energy deposition, Incident energy, Peak value, Most probable distribution (MPD)

CLC numbers TN25, O571.33

1 Introduction

At present, we need to know the difference of the energy deposition with γ-ray incidence on different materials[1]. We also want to find the best way to array the energy-absorption material of the detector so as to differentiate the incident energies accurately. In this paper, we have primarily done some simulations and analyses with different incident energies and geometrical models. We consider the most probable distribution (MPD) of energy deposition. Our expectation is that the peak values can take up as much share as possible, the distribution as narrow as possible, and can be reached as early as possible. Taking up more share and narrower distribution means higher precision of orienting energy and reaching the peak values early means less detector material.

2 Geant4 system

We have used a Monte Carlo program, GEANT4, which is a tool kit designed initially for simulating nuclear and high energy physics experiments, but in recent years has been used in a wide range of applications including radiation analysis, space and cosmic ray analysis and, more recently, medical oncology analysis and evaluations[2]. The tool kit is based on object-oriented technology. It provides transparency for the presentation of various physics parameters.

A set of models that describe the interaction of photons and electrons with matters at low energies has been implemented in the tool kit. The physical processes involved include photoelectric effect, Compton scattering, Raleigh effect, Bremsstrahlung, and ionization[3]. A low energy limit for particle interaction cor-

Supported by "Hundred People Plan Fund" of CAS

* Corresponding author: tangsb@mail.ustc.edu.cn

Received date: 2005-07-25

responding to the minimal energy within the validity range of the models is defined. A higher threshold for any specific application can be alternatively defined by the user.

Geant4 is supported by various operating systems[4]. In our simulation, we used the one supported by Linux (Redhat8). The simulation was run on dedicated Pentium-IV personal computers.

3 Models

The first geometry is a phantom irradiated by a monoenergetic photon point source (Water-Layer). The phantom has 200 slices of water and the slices are 0.5 cm thick cylinders with a 1 cm radius, along the central axis of the beam.

The second geometry is a phantom irradiated by a monoenergetic photon point source (Mix-Layer). The phantom has 100 slices with five layers, 6 cm of water followed by 3.5 cm of air, 1 cm of iron, another 3.5 cm of air, and the rest of water. The slices are 0.5 cm thick cylinders with a 1 cm radius, along the central axis of the beam.

The third geometry is a phantom irradiated by a monoenergetic photon point source (PSt-Layer). This model is similar to the Water-Layer except substituting water by polystyrene. We have chosen the plastic scintillation fiber (PSF) as the detecting material and the core of the fiber is made of polystyrene. The simulation of polystyrene will give some meaningful results for the geometrical configuration of the detector.

The fourth geometry is a phantom irradiated by a monoenergetic photon point source (Thin-PSt-Layer). The phantom has 200 slices of polystyrene and the slices are 0.05 cm thick cylinders with a 1 cm radius, along the central axis of the beam.

All the four geometries are shown in Fig. 1 except for some tiny differences in the second geometry and the fourth geometry. The SSD (source-to-surface distance) of all the four geometries is set to 100 cm. For the GEANT4 simulations, a total of 5×10^6 primary events are simulated for all energies [5]. The production threshold is set to 10 μm for all particles.

Considering the contribution per photon in the result, we have the energy deposition divided by the total of photons. In model 2, we even have the energy deposition divided by the mass of the corresponding material because the three materials in this model have large differences in the photon absorbance.

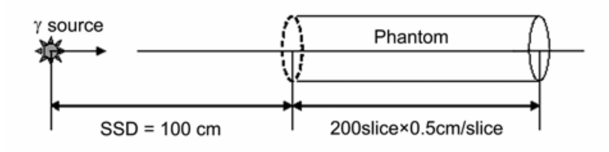

Fig.1 Geometrical structure of the models.

4 Results and discussions[6, 7]

4.1 Water-Layer model

We now first present the results for γ-ray radiation of model 1. Fig.2 shows the variation of energy deposition per photon with incident energy from the 1st slice to the 40th slice. As can be seen, the curve is smoother when the incident energy is lower. In the meantime, we can see that for different incident energies the peak values are different. When the incident energy is higher, the peak value is more apparent. In fact the peak value can take up more share when the energy is lower and the position of the peak moves left. This means that only fewer slices are needed to get the position of the MPD.

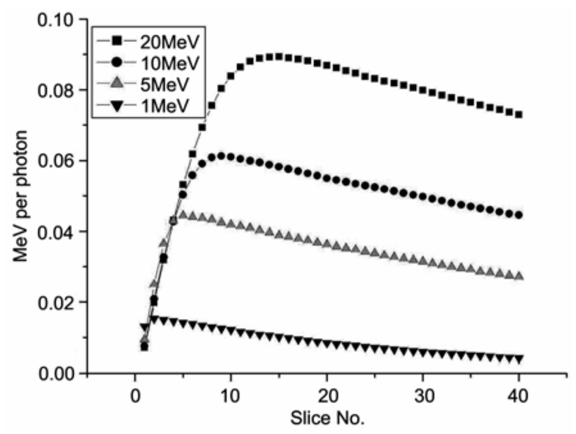

Fig.2 Energy deposition in Water-Layers for different incident energies.

4.2 Mix-Layer model

In Fig.3, we can see the energy deposition in Mix-Layers with the incident energy of 10 MeV. The curve shows a process of first rising and then falling when the incident photons move from low density material to high density material, i.e., from air to water. But, if the incident photons move from high density material to low density material, i.e., from water to air or from iron to air, the curves present only a simple falling tendency. This is in accordance with the theoretical analysis.

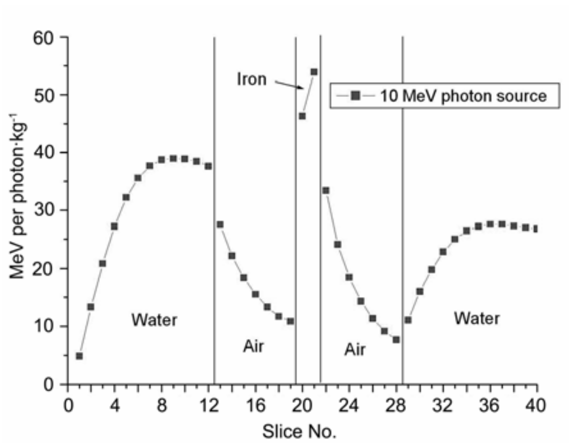

Fig.3 Energy deposition in Mix-Layers for 10 MeV incident energy.

When comparing the results of model 1 and model 2, we can get some conclusion. From Fig.4, we can see that the energy deposition of water slices of model 2 has a similar result to that of model 1.

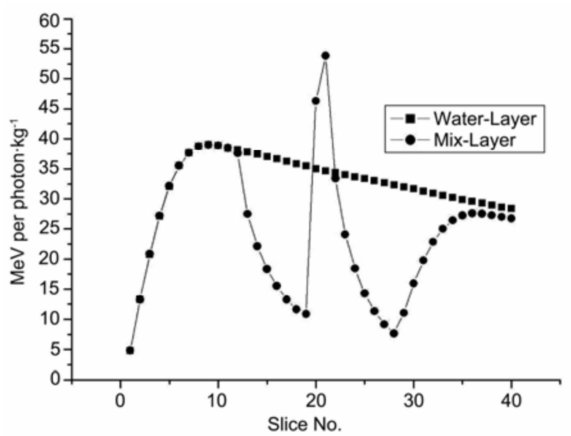

Fig.4 Comparison of energy deposition in Water-Layers and Mix-Layers for 10 MeV incident energy.

In fact, except for the middle 16 slices of other materials, the energy deposition of water slices of model 2 has only a constant difference compared to that of model 1. This is mainly because iron has a larger absorption coefficient of photons than water. Hence, we can insert iron slices (or other materials with large absorption coefficients) with certain thickness in certain positions to obtain a better most probable distribution (MPD) of energy deposition, which will not alter the shape of the curve. The resulting curve has a narrower distribution of energy deposition and the peak value can also be reached earlier.

4.3 PSt-Layer model and Thin-PSt-Layer model

We now present the results of model 3. Fig.5 shows the variation of energy deposition per photon with various incident energies in polystyrene from the first slice to the 40th slice. We can see the same situation as shown in model 1.

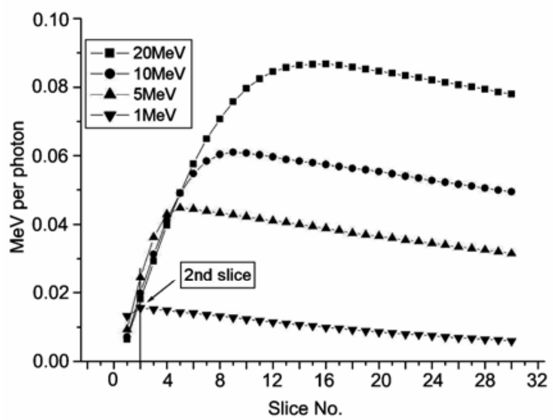

Fig.5 Energy deposition in PSt-Layers for different incident energies.

On the other hand, the curve has a relatively larger error when we choose 0.5 cm as the thickness of a slice for the incident energy of 1 MeV. The result was not obvious enough. Therefore, we chose 0.5 mm as the thickness of the slice for the lower incident energy such as 500 keV and 100 keV, as is done in model 4. In this model, we did some more accurate simulations with lower incident energy.

Next we present the results of model 4 in Fig.6. First we calculated only with the incident energy of 1 MeV. What was interesting was the position when the energy deposition reached the peak value. From Fig.5 of model 3, we can see that the curve reaches the peak in the 2nd slice, with the position of $2\times0.5\ \text{cm}=1\ \text{cm}$. While from Fig.6 of model 4, we can see that it reaches the biggest absorption in the 10th slice, with the position of $10\times0.5\ \text{mm}=5\ \text{mm}$. It means that when the incident energy is 1 MeV, the energy deposition reaches the peak at the thickness of 5 mm. We can even say that the peak is flat from the 5th slice to the 23rd slice and the length is $(23-5) \times 0.5\,\text{mm} = 9\,\text{mm}$. We successfully resolved the error of Fig.5 and got the position of the peak value.

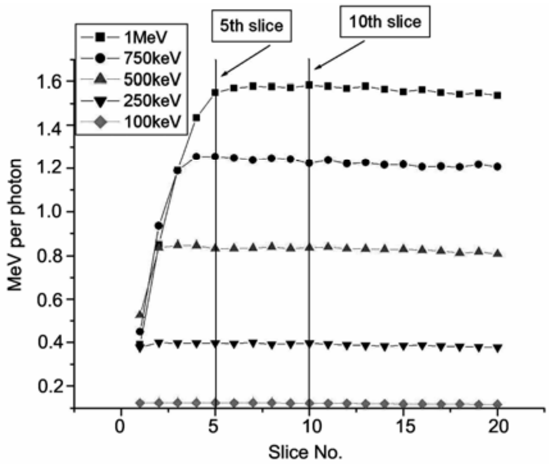

Fig.6 Energy deposition in Thin-PSt-Layers for different incident energies.

Also, we can analyze other incident energies in the same way and we can see that the peak value is not apparent any more when the incident energy is less than 500 keV. We can find that for an incident energy lower than 1 MeV, the curve becomes so smooth that the peak can hardly be found. So the configuration of detector will be more available when the incident energy is higher.

5 Conclusion

According to the interaction of γ-ray with matters, we know that for a certain photon, energy is lost only at some random layers. There is an MPD of energy deposition in which the detector has a bigger probability to detect the photons. We have got a series of meaningful results from these simulations. We can insert some large absorption coefficient slices with certain thicknesses in certain positions to obtain a better MPD of energy deposition, which will not alter the shape of the energy deposition. We will continue the simulation with the four models to get the best configuration. There should be very important results to the detector when applied in practice.

References

1 American Institute of Physics. Particle Physics Booklet, 1994, 225

2 Agostinelli S, Allison J, Amako K, *et al*. Nucl Instr Meth, 2003, **A506**: 250

3 Physics reference manual at the Geant4. Available from: http://geant4.web.cern.ch/geant4

4 Geant4 user guide. Available from: http://geant4.web.cern.ch/geant4

5 Carrier J F, Archambault L, Beaulieu L, *et al*. Med. Phys. 2004, **31**(3): 484-492

6 HBOOK user guide, CERN, Version 3

7 PAW—Physics Analysis Workstation, The Complete Reference, CERN, Version 1.07